JOURNAL OF NATURAL FIBERS
2024, VOL. 21, NO. 1, 2305228
https://doi.org/10.1080/15440478.2024.2305228

Weibull Statistic and Artificial Neural Network Analysis of the Mechanical Performances of Fibers from the Flower Agave Plant for Eco-Friendly Green Composites

Imen Lalaymia[a], Ahmed Belaadi[a], Messaouda Boumaaza[b], Hassan Alshahrani[c,d], Mohammad K. A. Khan[c,d], and Amar Dib[e]

[a]Department of Mechanical Engineering, Faculty of Technology, University 20 Août 1955-Skikda, El-Hadaiek Skikda, Algeria; [b]Laboratory of Civil and Engineering Hydraulic (LGCH), University 8 Mai 1945 Guelma, Algeria; [c]Department of Mechanical Engineering, College of Engineering, Najran University, Najran, Saudi Arabia; [d]Scientific and Engineering Research Centre, Deanship of Scientific Research, Najran University, Najran, Saudi Arabia; [e]Department of Mechanical Engineering, Faculty of Technology, Université Badji Mokhtar-Annaba B.P. 12, Annaba, Algeria

ABSTRACT

The research conducted focused on examining the unique properties of Agave Americana Flower Stem fiber (AAFS), particularly its behavior under quasi-static tensile conditions. A total of 200 AAFS fibers were subjected to tensile tests using a standard gauge length of 40 mm. Tests spanned seven groups with quantities (N) ranging from 30 to 200. The study aimed to understand the fibers' mechanical traits, as tensile resistance and modulus of elasticity, and to see how different test quantities influence these properties. A significant observation was the dispersion of the tensile characteristics of AAFS fibers, a common trait of natural fibers. To understand this, we applied rigorous statistical tools, including the Weibull distribution at a 95% confidence interval and one-way ANOVA. A mathematical model was produced utilizing data from experiments regarding the tensile behavior of AAFS fibers. The ANN provided correlation coefficients (R^2) of 0.9897, 0.9971, 0.9993, and 0.9939 for training, validation, testing, and all datasets respectively, which were able to accurately predict the experimental data. The proposed model would be of tremendous assistance to engineers and designers in obtaining green composite materials that are based on natural fibers and thereby more durable. These methods illuminated the patterns in our results, enriching our understanding of AAFS fiber mechanics.

摘要

本研究的重点是研究美国龙舌兰花茎纤维（AAFS）的独特性能，特别是其在准静态拉伸条件下的行为. 使用40 mm的标准标距长度对总共200根AAFS纤维进行拉伸试验. 测试分为七组，数量（N）从30到200. 这项研究旨在了解纤维的力学特性，如抗拉强度和弹性模量，并了解不同的测试量如何影响这些性能. 一个重要的观察结果是AAFS纤维的拉伸特性的分散，这是天然纤维的一个常见特性. 为了理解这一点，我们应用了严格的统计工具，包括95%置信区间的威布尔分布和单因素方差分析. 利用有关AAFS纤维拉伸行为的实验数据建立了数学模型. 人工神经网络对训练、验证、测试和所有数据集的相关系数（R2）分别为0.9897、0.9971、0.9993和0.9939，能够准确预测实验数据. 所提出的模型将极大地帮助工程师和设计师获得基于天然纤维的绿色复合材料，从而更耐用. 这些方法阐明了我们结果中的模式，丰富了我们对AAFS纤维力学的理解.

KEYWORDS

Agave americana; tensile behavior; statistical methods; Weibull statistic; hazard function

关键词

美洲龙舌兰; 拉伸行为; 统计方法; 威布尔统计; 危险功能

CONTACT Ahmed Belaadi ahmedbelaadi1@yahoo.fr; a.belaadi@univ-skikda.dz Department of Mechanical Engineering, Faculty of Technology, University 20 Août 1955-Skikda, El-Hadaiek Skikda 21000, Algeria

Introduction

Natural fibers are becoming more crucial in the packaging industry and in the manufacture of biocomposites (Rice et al. 2019) because of their environmentally responsible practices in production and consumption, recyclability capacities, and the added value they provide as part of the circular organization (Sanjay et al. 2018). Synthetic fibers made of carbon, glass, aramid, and ceramic are particularly expensive, hazardous, and unsustainable; prolonged exposure can also endanger human health (Indran and Edwin Raj 2015). The use of natural fibers is primarily driven by a concern for both the environment and the economy (De Rosa et al. 2010). As reinforcement for biocomposites, various types of plant fibers including *Jancus efusus* (Maache et al. 2017), *Ageratina adenophora* (Selvaraj, Chapagain, and Mylsamy 2022), *Myriostachya wightiana* (Parida, Kumar Pradhan, and Kumar Pandit 2023a), *Yucca Treculeana* (Belaadi et al. 2022), and *Albizia amara* (Senthamaraikannan et al. 2019) are brought in use. Natural fibers, such as fibers of *Agave americana*, which are made of lignocellulosic materials, have proven to be excellent candidates for use as a reinforcement in biocomposite materials (Van de Velde and Kiekens 1999). Organic strands, however, have a higher absorption rate of moisture. Because they are hydrophilic, they deteriorate at the interface between the matrix and the fiber. As the insertion of absorbent fibers into a hydrophobic matrix is not straightforward, it is essential to improve the adhesion of biocomposites by chemical means to enhance their performance due to low fiber/matrix adhesion (Fiore, Scalici, and Valenza 2018). Additionally, the anatomical characteristics of fibers vary between species, which affects their density and mechanical characteristics. The size and quality of natural fibers are influenced by a number of variables, including fiber extraction, storage time, and environmental conditions (Gahgah et al. 2023). According to Belaadi, Bourchak, and Aouici (2016), the gauge length (GL), equal to 20 mm, and the number of trials ($N = 15$ to 40 trials) affect the mechanical properties of sisal fibers. They also noticed that the sisal fiber was very anisotropic, which prompted them to estimate the elastic characteristics of this fiber using the Weibull distribution with two and three parameters and various (index of probability) estimators. Dembri et al. (2022) performed a study on the mechanical characteristics of untreated *Washingtonia Filifera* (WF) fiber across five test batches. The data demonstrated an improvement in mechanical characteristics as the number of batches grew from 30 to 150. According to statistical analysis, Kaplan–Meier's estimator best fits the WF fiber, particularly in the 120 tests batch which was found to be the best performer. A one-way analysis (ANOVA) indicated that WF yarns' mechanical characteristics are dependent on the test quantity. Gahgah et al. (2023) delved into the effect of test number (N) on elementary sisal yarn mechanical properties, concentrating on modulus of elasticity (E), tensile stress (σ), and rupture strain (ε). After performing static tensile tests over five distinct sets (20, 40, 60, 80, and 100 tests), they found a consistent decline in σ and ε of the sisal yarns as N grew from 20 to 80, with values stabilizing between 148 MPa and 138 MPa for stress and 8.41% to 7.15% for strain at break. A notable drop was recorded for $N = 100$ tests, where the values descended to stress at 135 MPa and break strain at 6.70%. This study revealed that the yarn exhibited optimal mechanical properties at $N = 100$ tests. In terms of modeling the mechanical characteristics, the distribution 2P-Weibull-LS (least square) proved more reliable as compared to the method ML (maximum likelihood). Further, through analysis with a one-way ANOVA, the pivotal influence of N on the mechanical attributes of the sisal yarn was underscored. Gahgah et al.'s findings hold potential significance for the advancement of durable ropes and composite structures, fostering progress in design, performance, and the creation of innovative materials and methodologies in related sectors. A statistical model was developed by Wang et al. (2022) to investigate the behavior of uncertainty tension for 30 threads of jute fiber of 100 mm gauge length (GL), taking into account the impacts of property distribution and fiber crimp. A probability distribution function pertaining to the beta function for fiber strain was utilized to depict the statistical characteristics of the crimped jute fibers. While the yarn strength and effective modulus of elasticity had a normal distribution, the tensile plots of comparable yarn samples displayed features that were in line with the beta distribution observed in crimped strain. With reference to the variability in the nonlinear tensile behavior of jute fibers, this observation may make forecasts more accurate. Tensile properties for 13 sets from 30 raw and processed jute yarn specimens having surface twist angles varying from 11° to 13° and a 267 tex linear density measured with GL = 50 mm have been statistically characterized by Saaidia et al. (2017).

Different NaOH (sodium hydroxide) concentrations and immersion times were applied to the jute yarns. For the statistical analysis, Weibull approaches with two and three parameters were employed. The results show that there is variation in the failure strain, stress, and modulus of elasticity in uniaxial tensile strands, which is largely influenced by immersion period and concentration of NaOH. Optimal mechanical characteristics were attained with an immersion period of 2 h and a 2% NaOH dosage. Belaadi, Amroune, and Bourchak (2019) investigated the impact of the sodium bicarbonate ($NaHCO_3$) on vegetal flax fibers mechanical characteristics. Their focus was on crucial mechanical attributes like tensile stress, break strain, and modulus of elasticity. The study found that a 20% $NaHCO_3$ treatment over a period of 120 h enhanced the fibers" mechanical performance. Specifically, there was a 43% increase in tensile strength and an 81% rise in Young's modulus relative to the untreated samples. The researchers employed the Weibull distribution for their analysis, which indicated marginally elevated values for the chemically treated fibers. An ANOVA assessment was also conducted, confirming the significant influence of varying $NaHCO_3$ concentrations on flax fiber mechanical behavior. With a gauge length, GL = 40 mm baseline length, the average mechanical characteristics of the fibers (WF) were found to be 119.3 ± 86.28 MPa for tensile strength, 20.55 ± 11.08 for ultimate strain, and 2.34 ± 1.36 GPa for Young's modulus. A SEM (scanning electron microscope) analysis of various Washingtonia biomasses was conducted recently. They came to the conclusion that Washingtonia fiber holds a great deal of promise for use as a biomaterial in the future for a variety of purposes. Amroune et al. (2020) explored the influence of gauge length on the mechanical attributes of flax fibers, specifically UTS, modulus of elasticity and failure strain. The research discovered that as gauge length increased, there was a reduction in fiber stress and strain at break. Anisotropic properties were evident in the flax fibers, corroborating previous studies on jute fibers. The 2-parameter Weibull model closely mirrored the experimental results compared to the 3-parameter version. Notably, flax fibers tested at different gauge lengths (50 mm vs. 30 mm) showed varied modulus values. The study emphasizes the importance of gauge length in evaluating flax fiber mechanics and recognizes the 2-parameter Weibull model as an effective analytical approach.

For optimal use of *Agave americana* fibers in load-bearing applications, a direct assessment of their mechanical properties is essential. While there is ample research on synthetic fibers, using statistics techniques that evaluate natural fibers' mechanical traits is still in its infancy (Lalaymia et al. 2023). The primary goal of this study is to examine the tensile behavior of fibers from Agave americana flower stalk samples that vary in size. In this study, two-parameter Weibull statistics along with ML and LS prediction approaches are used to investigate the tensile properties of 200 AAFS fiber samples as the first time. The authors state that this is the first evaluation of this new fiber for samples of different sizes. Additionally, a thorough artificial intelligence prediction was performed for this fiber's tensile characteristics, which were then compared with available data.

Materials and methods

Extraction of fibers

The *Agave americana* is a succulent native to Mexico, and its presence has been felt globally, even in semi-arid and arid regions like Ain Achir in Annaba, Algeria. This plant stands as a unique species in the Agavaceae family and is a part of the Agavoideae subfamily. It is well regarded for its potential in the realm of sustainable material production. When mature, the agave can rise to an awe-inspiring height of 30 feet, characterized by its lengthy floral spike adorned with bright yellow or greenish-yellow blossoms. However, post-flowering marks the end of its life cycle, leaving behind only the robust flower stalk, which is usually discarded. To extract fibers from these Agave americana flower stems (AAFS), they are first peeled and sectioned into 50 cm pieces. Subsequent immersion in water at temperatures between 30°C and 35°C for a period of 30–45 days facilitates their breakdown. The environment is ripe for anaerobic bacterial activity, hastening the biological decomposition of the stalk and aiding fiber extraction. Once this phase concludes, the fibers are separated from the stalks by hand, washed, and set out to air dry (Lalaymia et al. 2023).

Mechanical testing and SEM micrographs

These extracted fibers are then fixed to a paper frame measuring 30 mm in width and 100 mm in height (Figure 1). A rectangular hole, 10 mm by 30 mm, is present at the frame's center, setting the gauge's length (GL) at 20 mm (Figure 1c, d). The framework is then positioned into the testing apparatus jaws. The mechanical properties of AAFS fibers, including tensile resistance, modulus of elasticity, and break strain, are evaluated as per the standards ASTM D 3822-07 with a 40 mm gauge length (Belaadi, Amroune, and Bourchak 2019).

For detailed measurements, an optical magnifier from ZEISS equipped with a Plan-Achromat 400 lens is used. To determine the average diameter of each fiber, measurements are taken at three random points along its length for all 200 samples (Lalaymia et al. 2023). To take in-depth photos of the AAFS fibers, a scanning electron microscope, or SEM, was used. To be more precise, settings for magnification and accelerating electron voltages between 3 and 5 kV were applied to the MEB-FEG Quattro S microscope. The fibers were coated with gold to increase electrical conductivity and decrease surface charging effects, which improved the imaging quality. The size, shape, and physical attributes of the AAFS fibers, as well as their microstructure, were revealed by this sophisticated imaging method. A thorough grasp of the fibers' morphology was made possible by using the SEM, particularly in its topographic mode, which was crucial for determining how the fibers affected mechanical properties and SEM micrographs were captured (Figure 1c, d).

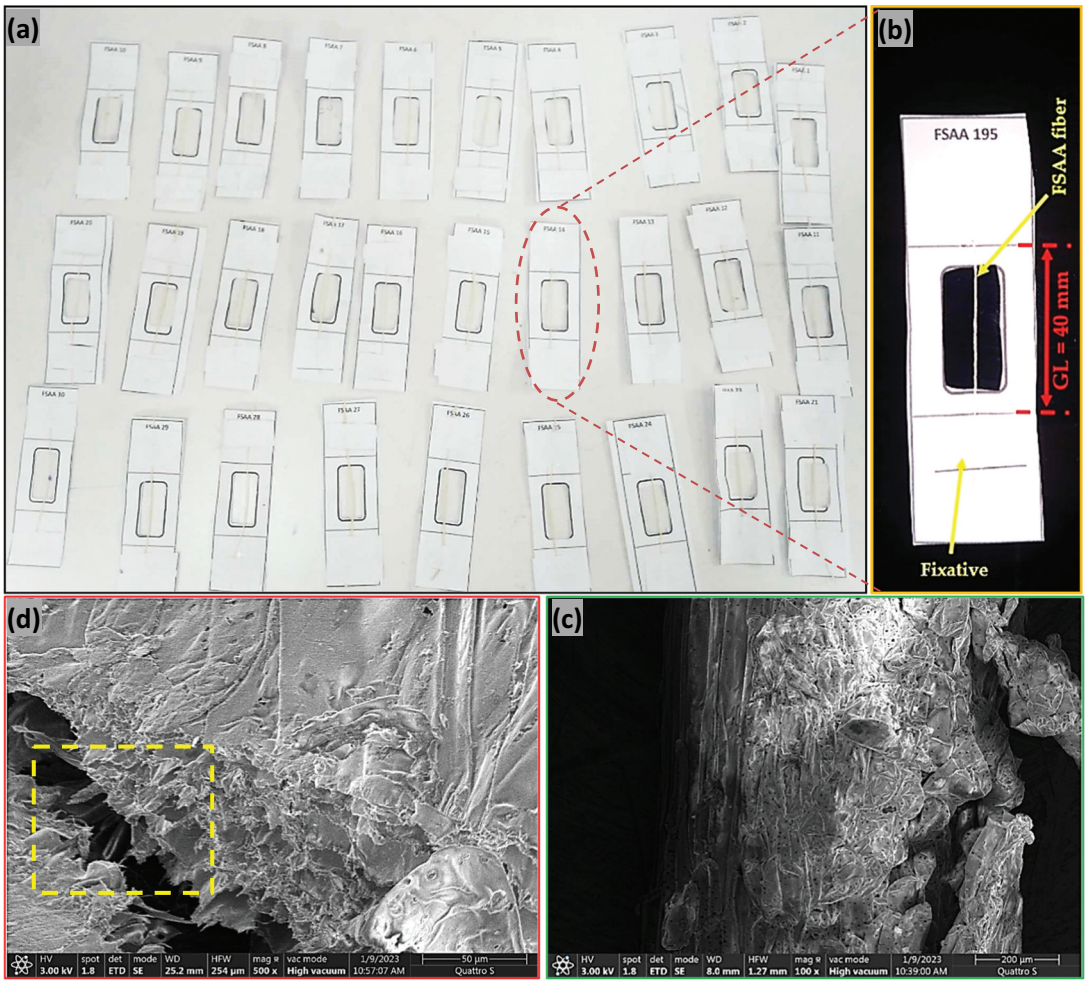

Figure 1. (a) Preparation of AAFS fibers for tensile testing, (b) detail of a single fiber placed and glued in paper, (c) topographic surface of single AAFS, and (d) fiber microfibrils of AAFS fiber.

Weibull statistical analysis

The Weibull model, which takes the randomness of the data into account, is frequently used in fragile materials in which the distribution of damage plays an important role in the failure of the material (Dembri et al. 2022). However, several investigations have also applied similar formulation to the situation of carbon fibers (Belaadi, Amroune, and Bourchak 2019) and bundles of glass fibers. Additionally, even if its use is documented in the literature (Elsayed 2008), the decision to utilize a model to depict the distribution of the strength at failure in ductile polymer composites such as PET (Polyethylene terephthalate) fibers deserves justification. Kolmogorov–Smirnov test is used to determine if the tensile strength samples fit a Weibull law (Lapidot 2020). The Gauss Laplace law is a normal distribution of continuous probability, which is dependent on variables. The first parameter (μ) mean, provides details on the distribution's center Standard deviation (SD), providing dispersion information, is a second parameter (δ). Equation (1) (Virk, Hall, and Summerscales 2010) defines the probability density function (PDF) as Gaussian (normal). There is a probability density associated to this variable ($\mu = 0$, $\delta = 1$), which is given by Equation (2). The normal centered reduced variable equals $y = (x-\mu)/\delta$. Furthermore, if $\lambda > 0$, we obtain Equation (3) for the density function and the log-normal distribution (LND) as defined with ξ (scaling parameter) and (parameter of location). The natural logarithm arithmetic average of the mechanical characteristics is represented by ln(x), while their standard deviation is represented by ξ (Belaadi, Amroune, and Bourchak 2019).

The cumulative distribution function (CDF), commonly referred to as the density probability function of the Weibull distribution with three parameters, is described by Equation (4) (Amroune et al. 2020; Belaadi, Amroune, and Bourchak 2019). The Weibull model, which posits that a fiber fracture results from the failure of its weakest component, can frequently and successfully simulate the mechanical characteristics of fibers (Janis Andersons et al. 2005). With $s_{0=0,}$ Eq. 5 takes on Eq. 5. After Equation (5) has been simplified, Equation (6) can be used to explain the probability of two-parameter Weibull survival F(x), supposing the threshold to be zero ($s_{0=0,}$) (Virk, Hall, and Summerscales 2009). The least squares estimate (LS) can be used to calculate the variables m, s, and s_0. The above equation is rearranged and written as (Estrada, Linero, and Ramírez 2013) ((Equation (7)).

$$P(x|\ \mu\ ,\alpha) = \frac{1}{\sqrt{2\pi}s} e^{-\frac{1}{2}\left(\frac{x-\mu}{\alpha}\right)^2} \tag{1}$$

$$\varphi = \frac{1}{\sqrt{2\pi}} e^{-\frac{y^2}{2}} \tag{2}$$

$$P(x\ |\xi\ ,\lambda\ ) = \frac{1}{x\xi\ \sqrt{2\pi}} e^{-\frac{1}{2}\left(\frac{\ln(x)-\lambda}{\xi}\right)^2} \tag{3}$$

$$F(x|\ s_0, s, m) = 1 - e^{\left[-\left(\frac{x-s_0}{s}\right)^m\right]} x \geq s_0 \tag{4}$$

$$F(x\ |s, m) = \frac{m}{s}\left(\frac{x}{s}\right)^{m-1} e^{\left[-\left(\frac{x}{s}\right)^m\right]} \tag{5}$$

$$F(x\ |s, m) = 1 - e^{\left[-\left(\frac{x}{s}\right)^m\right]} \tag{6}$$

$$\ln\left[\ln\left(\frac{1}{1-\mathrm{P}}\right)\right] = \mathrm{m}\ \ln(\mathrm{x}) - \mathrm{m}\ \ln(\mathrm{s}) \tag{7}$$

where s_0, a location parameter, reflects the parameter × mean value (minimum lifetime), $s > 0$ is the parameter scale (typical value) and m is the parameter shape, also known as the Weibull modulus, are

all real positives ($R > 0$). Additionally, the parameter s_0 in our study indicates the distinctive mechanical characteristics, specifically σ_0, ε_0, and E_0, which are, respectively, distinctive tensile stress, failure strain, and the modulus of elasticity. The form $\ln\left[\ln\left(\frac{1}{1-p}\right)\right] = f(\ln(x))$ if the Weibull model is applied, then the data is represented linearly. When we represent this formula, we get a line with a slope of m. After that, it is feasible to determine the parameter s thanks to the ordinate at the line's origin. Finding an estimate of P (probability of survival) using this method is challenging. As a result, the empirical index (probability index) or other estimators can be used to determine the value of Pi(x) for the rank sample i. The estimator's overall formula is: $p_{i=\frac{i-\alpha}{n-\beta}}$ where $\alpha = 0.03$, 0.375, and 0.5 and $\beta = 0$, 0.25, 0.4, 1. In the literature, four estimators have often been utilized (Morris 2003). For sample populations larger than 20, the first estimator $p_{i=\frac{i}{n+1}}$ was most frequently utilized. Recent research, however, have demonstrated that it skews scores further than the estimator $p_{i=\frac{i-0.5}{n}}$. This second estimate will be applied in the present investigation because it is best suitable with population groups ranging from 20 to 50. However, populations of samples less than six are handled by the estimator 3 $p_{i=\frac{i-0.3}{n+0.4}}$, whereas populations of samples less than 10 are handled by the estimator 4 $P_i = \frac{i-0.375}{n+0.25}$.

The maximum likelihood (ML) approach is another technique for estimating the Weibull probability's parameters and is represented by the following formula ((Equation (8)). The ML is a powerful estimating method that possesses amazing mathematical traits like regularity. The goal of this strategy is to identify the variables that will increase the likelihood of sample populations. In other words, this estimation technique is favored statistically due to its strength. Additionally, it enables straightforward confidence interval creation, which results in the automatic estimation of Weibull parameter uncertainty at a 95% CI.

$$Likelihood(m, slx_1, \ldots\ldots\ldots\ldots..x_2) = \prod_{i=1}^{n} F(x_i) = \prod_{i=1}^{n} \frac{m}{s}\left(\frac{x_i}{s}\right)^{m-1} e^{\left[-\left(\frac{x}{s}\right)^m\right]} \tag{8}$$

In this study, Minitab software version 16 was employed. While there are a number of alternatives to estimate the Pi index and select the statistical methodology (LS vs. ML), Minitab makes use of some commands and functions that produce an adjusted statistic (Abbasi et al. 2011).

Artificial Neural Network (ANN)

An approach that can be used to simulate, examine, and predict the response for a variety of input parameters is artificial neural network (ANN). As a result, the present research uses ANN to combine various input variables and predict the output. Three stages go into creating a model from experimental data: training, confirmation, and examination. This network functions similarly to the human mind, which is capable of learning accurately from the available information without providing any formulas, making it useful for solving nonlinear and complex issues. The three layers of an ANN are typically comprised of a data input, an outcome, and a hidden layer. Neuronal components vary in number within each layer (Mulenga, Ude, and Vivekanandhan 2021). Since the general goal is to obtain a result that corresponds precisely to the input variables, signals pass first through the initial input layer, then through the hidden layers and lastly via an output layer. The learning process provides the information exchanged across the neurons or linked node. The model was trained and tested using the MATLAB software program (Ornaghi, Motta Neves, and Monticeli 2021).

Results and discussion

Tensile properties of AAFS fiber

AAFS fibers were tensile tested in an ambient environment at 1 mm/min. The fibers were distributed in seven batches containing 30 samples each, resulting in an aggregate of 200 randomly chosen

elementary fibers from a particular lot, all of which were measured at GL = 40 mm. Figure 2a shows the stress–strain results of these 30 AAFS fibers test. Notably, the wide range of variability present in natural fibers emphasizes the necessity of thorough statistical analysis. Similar patterns were observed in *Washingtonia Filifera* (Dembri et al. 2022). In Figure 2a, a thorough statistical study is obviously necessary given the wide range of outcomes, a phenomenon unique to natural fibers. For flax fibers, this behavior was noted at GL = 20 mm in the studies by Belaadi, Amroune, and Bourchak (2019). In Figure 2b, the strength–deformation relationship of AAFS fibers under tensile stress is illustrated. This curve highlights a two-phase behavior typical of cellulosic fibers. Initially, as tension is applied, the fiber exhibits a nearly straight-line response, representing the fiber's overall stretch and the internal realignment of its microscopic structures called fibrils. As the test progresses, the fiber resists the pull with a more pronounced straight-line behavior right up until it breaks. Interestingly, just before the breaking point, the fiber shows a brief period of increased resistance or elasticity, suggesting its inherent resilience against the applied force. The first phase, which represents a non-linear zone for strains between 0% and 0.8%, is followed by the second phase, which is represented by a dramatic fall

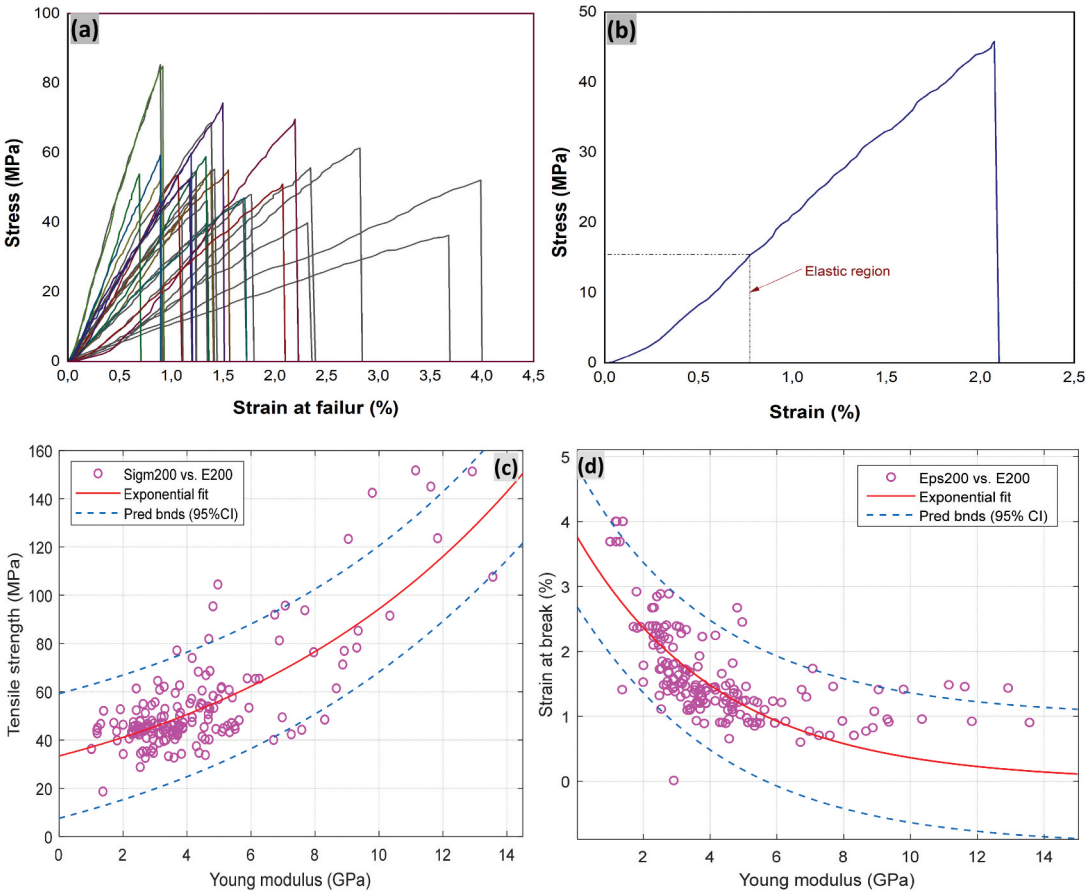

Figure 2. Stress–deformation graphs (a) of the first 30 AAFS fibers and (b) representative behavior for a GL = 40 mm tensile test, (c) dispersion graphs of the 200 AAFS fiber trials tensile deformation versus modulus of elasticity, and (b) tension resistance versus modulus of elasticity.

Table 1. Average, covariance, and standard deviation values of the AAFS fibers mechanical characteristics under static tensile testing in this study.

	Strain (%)			Stress (MPa)			Modulus of elasticity (MPa)		
N	Average	SD	CV	Average	SD	CV	Average	SD	CV
30	1.652	0.779	47.15	53.52	12.07	22.55	4.161	1.903	45.73
60	1.611	0.646	40.15	54.31	18.43	33.93	4.079	2.018	49.47
90	1.528	0.606	39.65	51.59	17.2	33.33	4.107	1.948	47.43
120	1.564	0.672	42.99	50.13	15.36	30.64	3.945	1.828	46.33
150	1.557	0.655	42.05	52.72	18.26	34.63	4.203	2.176	51.77
180	1.586	0.676	42.61	53.94	21.75	40.32	4.268	2.36	55.29
200	1.598	0.700	43.83	53.73	20.85	38.80	4.252	2.313	54.39

in stress at a mean value of 45.92 MPa, corresponds to the failure of the specimen. The elastic region on the graph was used to calculate the modulus of elasticity for strains between 0.3% and 0.8%.

Table 1 presents standard deviation (SD) and average values of the tensile parameters, such as break strain, stress, and modulus of elasticity, derived from 200 tests of AAFS fiber at different test numbers (N). Table 1 shows notable dispersions of the mechanical characteristics. For the seven clusters of the investigated samples ($N = 30$, 60, 90, 120, 150, 180, and 200), the values obtained for the CVs of ε, σ, and E are in fact (47.15, 40.15, 39.65, 42.05, 42.61, and 43.83%), (22.55, 93.33, 33.33, 30.64, 34.63, 40.32, and 38.80%), and (45.73, 49.47, 47.43, 46.33, 51.77, 55.29, and 53.39%), respectively. In Table 1, we can see how testing number affects AAFS fiber mechanical strength. For instance, when comparing a group of 30 tests to a group of 180 tests, there were changes in average values: σ decreased from 53.52 ± 12.07 to 53.94 ± 21.75 MPa, ε changed from $1.65 \pm 0.77\%$ to $1.59 \pm 0.67\%$, and E slightly increased from 4.16 ± 1.90 to 4.27 ± 2.36 MPa.

We compare the results of research on natural fibers published in the literature. Because of the various parameters influencing vegetable fiber production, the comparison of their mechanical characteristics is difficult. The σ, ε, and E values obtained in this work surpass those found in previous research (Benzannache et al. 2021; Bezazi et al. 2014; Dembri et al. 2022; Ferfari et al. 2023; Lekrine et al. 2022; Parida, Kumar Pradhan, and Kumar Pandit 2023b). This is because previously there were fewer tests conducted than in our study, which involved 120 samples. For σ, ε, and E, for AAFS fibers, the experimental findings were 50.73 MPa, 1.59%, and 4.25 GPa, respectively. In this study, AAFS fiber with a gauge length of GL = 40 mm was found to have a higher tensile stress than *Myriostachya wightiana* fiber (46.554 MPa) (Parida, Kumar Pradhan, and Kumar Pandit 2023a), and lower than that of *Juncus effusus* fiber (113 ± 36 MPa) (Maache et al. 2017). The measured gauge lengths are 20 and 40 mm, respectively.

Statistical analysis of AAFS fiber data

Due to the diversity of the mechanical properties of plant-based cellulose fibers, it is difficult to design composite structures. To appreciate the advantages of biocomposites, or threads formed from vegetable fibers, understanding the factors that improve their performance is essential. A 95% CI predictive performance model is used in Figure 2c, d to illustrate the variation in the link between the power fit, Young's modulus, and tensile strength vs. rupture strain. The modulus of elasticity decreases as the resistance increases, as is illustrated above, also a similar trend is observed in the relationship between rupture strain and modulus of elasticity (Gahgah et al. 2023). According to different distribution methods, the experimental histograms of mechanical characteristics are shown in Figure 3a–c, specifically for tests $N = 200$. We used the normal square root rule, taking into account the quantity of data to be analyzed, to choose the cells needed for the histogram. There are several statistical distributions available in the subject of material science; the three most commonly used in material research to characterize different material properties are the normal distribution, the Weibull distribution, and the

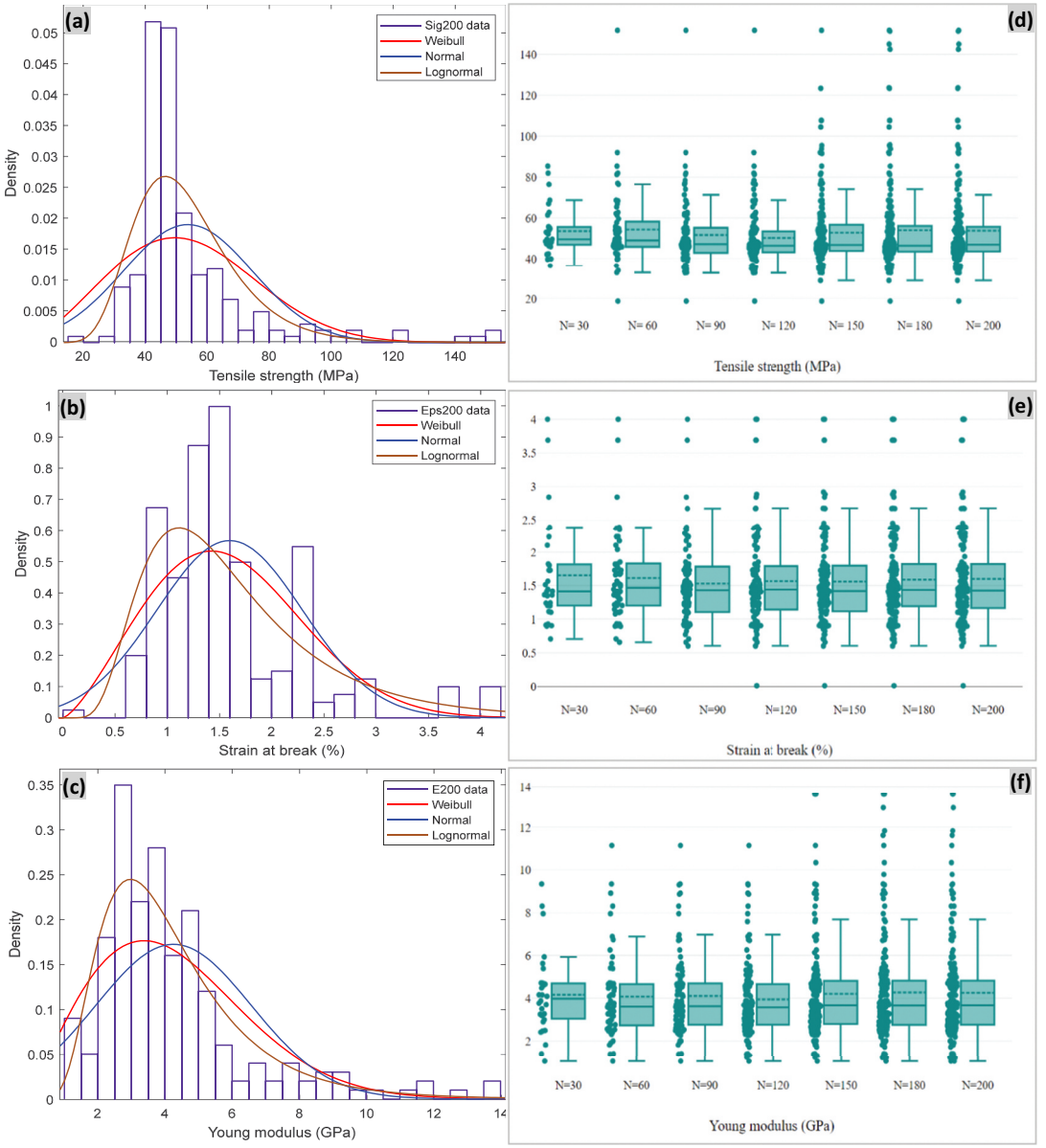

Figure 3. (a-c) Histograms of AAFS fiber tensile properties data with estimated Weibull, normal and lognormal density functions for $N = 200$ and (d-f) mean tensile characteristics as a function of trial number N.

lognormal distribution. Indeed, the Weibull distribution is widely used for resistance prediction as well as for assessing fragile rupture, whereas the use of lognormal distribution is limited to represent the particle size and cracking of material. However, the normal distribution is a flexible distribution that may be utilized to characterize random phenomena and mimic a variety of material properties.

Tukey plots showed the mean AAFS mechanical properties, such as strain, modulus of elasticity, and tensile strength, varying with sample number (Figure 3d–f). The box diagrams employed display the overall patterns of the group responses. The distribution of responses and additional features,

including mechanical characteristics of a group's responses, can be shown graphically in box plots. In Figure 3(d–f), AAFS fibers' mean mechanical characteristics vary as a function of sample number. These parameters are represented by Tukey plots (box plots). Quantiles (Q1 and Q3), the maximum, minimum, median, and median of the variable values constitute this representation. As an example, the median, Q1, Q3, minimum and maximum values of the samples for $N = 120$ are (46.35, 42.85, 53.47, 18.67, and 151.37 MPa) for stress, (1.43, 1.13, 1.79, 0.01, and 4.02%) for strain, and (3.57, 2.75, 4.66, 1.09, and 11.14 GPa) for Young's modulus.

Kolmogorov–Smirnov and normality trials

Kolmogorov–Smirnov method was utilized to perform a series of normalcy tests as part of our inquiry into the material qualities of AAFS fibers. Table 2a shows a significant p-value of 0.010 in the results for the constraint of AAFS fibers. Since this result is less than the traditional cutoff of 0.05, the assumption of a normal distribution of data is rejected. This indicates that the natural fiber constraint data is not regularly distributed. Furthermore, 2.62 was found to be the skewness parameter for this dataset. This level of positive skewness indicates a strongly skewed distribution to the right. This implies that in AAFS fibers, there are more occurrences of extraordinarily high constraint values than in low ones. Additionally, comparable non-normal patterns were found in the break strain and modulus of elasticity. With p-values of 0.010, both parameters showed substantial deviations from normalcy. A positive skewness was also shown by their respective skewness values of 1.40 for break strain and 1.79 for modulus of elasticity. This corroborates the finding that AAFS fibers can show very high values for break strain and modulus of elasticity. When combined, these results have significance for the investigation and application of these organic fibers. These important metrics have a non-normal distribution, which might affect the choice of relevant statistical studies and offer a more complex understanding of the intrinsic AAFS fibers. Therefore, a Weibull distribution as well as a lognormal distribution can all be used to characterize the property dispersion. Thus, it is imperative to ascertain which of these three principles most accurately characterizes the outcomes of the experiment.

The Anderson–Darling test findings for various distributions applied to a material's tensile resistance, failure strain, and modulus of elasticity are shown in Table 2b. The p values below 0.05 show that there were substantial deviations from every distribution seen overall. With an AD value of 8.350, the lognormal distribution turns out to be the best fit for the tensile resistance. Likewise, failure strain and modulus of elasticity showed AD values of 1.347 and 4.581, respectively, and were also in close alignment with the lognormal distribution. In later investigations, care is recommended since,

Table 2. Normality test for N = 200 tests according to Kolmogorov–Smirnov criteria estimates of p values and AD of various distributions using N = 200 trials.

a-Normality test values			
Skewness parameter	0.010	0.010	0.010
p-value	2.62324	1.40709	1.79294

b-Estimates of p values and AD various

	Tensile Strength (MPa)		Strain At Failure (GPa)		Young Modulus (%)	
Distribution	*AD*	*p*	*AD*	*p*	*AD*	*p*
Normal	17.038	0.005	6.855	0.005	9.454	0.005
Lognormal	8.350	0.005	4.581	0.005	1.347	0.005
Weibull	17.802	0.010	5.438	0.010	5.831	0.010
3P – Weibull	13.311	0.005	5.541	0.005	3.386	0.005

although certain distributions more closely resembled specific material qualities, none offered an ideal approximation for any of the characteristics.

AD adjustment quality of AAFS fiber normality data

The intricacies in the data become more apparent as the AAFS fiber properties are analyzed across several distributions. The lognormal distribution is frequently found to be the most suitable for tensile strength; this is especially true for sample sizes of 200, as seen by its AD value of 8.350. The strain at break displays a varying agreement with distributions; for sample sizes of 120, in particular, the lognormal is prominent with an AD value of 4.665. When evaluating Young's modulus, the data indicates a clear trend: the AD values for the normal distribution progressively grow with sample size, reaching a peak of 9.454 for a sample size of 200. On the other hand, the behavior of the lognormal and 3P-Weibull values varies with size. Interestingly, with 200 samples, the lognormal achieves an AD value of 1.347, indicating that it may be a suitable descriptor. All together, these findings highlight how complex the material's properties are, with the lognormal distribution typically providing the most accurate depiction across a variety of parameters. The information emphasizes the necessity of a comprehensive strategy that strikes a balance between statistical and empirical insights when analyzing AAFS fiber properties. Table 3 shows the estimates of AD adequacy across the various distributions ($N = 30, 60, 90, 120, 150, 180, 200$).

The AAFS fiber strength, strain, and modulus of elasticity were examined in this work by using the Weibull function with two, which showed a considerable degree of variance. Based on Weibull-LS and ML, nevertheless, it is perceived that the two-parameter Weibull lines for both the LS and ML estimation methods (Figures 4) for the AAFS fiber appear to have a reasonable fitting line. The experimental values fit in a quasi-linear fashion, with a slight offset from one another. This behavior has been reported by Belaadi, Bezazi, Maache, et al. (2014) in the case of sisal fiber and by Bezazi et al. (2014) for *Agave Americana* fiber. The statistics results for the two-parameter Weibull distributions are shown in and Figure 4 and Table 4, respectively.

These are measured using five different estimators: Modified Kaplan–Meier, Mean Rank, Median Rank, and Kaplan–Meier (Andersons, SparniņŠ, and Poriķe 2009). Weibull modulus fit and variability are explained by correlation coefficient R^2 values. The correlation R^2 varies from 0.863 to 0.939 for tensile strength, from 0.842 to 0.97 for strain at break, and from 0.957 to 0.987 for Young's modulus based on Table 6 and the 2P-Weibull analysis. Upon closer inspection, the Kaplan–Meier estimator stands out from the others since it consistently displays the highest R^2 correlation coefficient among these estimators.

Table 5 presents the parameters, forms, and defining values for the Weibull distribution of each mechanical property. For the 2P-Weibull-ML model regarding deformation (m_ε), strength (m_σ), and

Table 3. Estimates of AD adequacy based on various distributions.

	Tensile stress (MPa)				Break strain (GPa)				Modulus of elasticity (GPa)			
N	Normal	Log-normal	Weibull	3P-Weibull	Normal	Log-normal	Weibull	3P-Weibull	Normal	Log-normal	Weibull	3P-Weibull
30	1.291	0.708	1.568	0.510	1.537	0.389	1.164	0.398	0.774	0.474	0.565	0.471
60	3.668	1.823	4.366	3.369	1.484	0.274	1.343	0.447	2.006	0.301	1.257	0.708
90	4.358	1.766	5.276	3.607	1.938	0.357	1.773	0.554	3.143	0.398	2.115	1.193
120	6.966	3.227	8.907	6.381	3.327	4.665	2.897	2.954	3.930	0.602	2.805	1.595
150	9.869	4.449	10.480	7.587	4.160	4.573	3.516	3.601	6.695	0.915	4.468	2.572
180	17.038	8.350	16.368	12.372	5.498	4.552	4.540	4.638	9.395	1.386	5.843	3.363
200	17.038	8.350	17.802	13.311	6.845	4.435	5.438	5.541	9.454	1.347	5.831	3.386

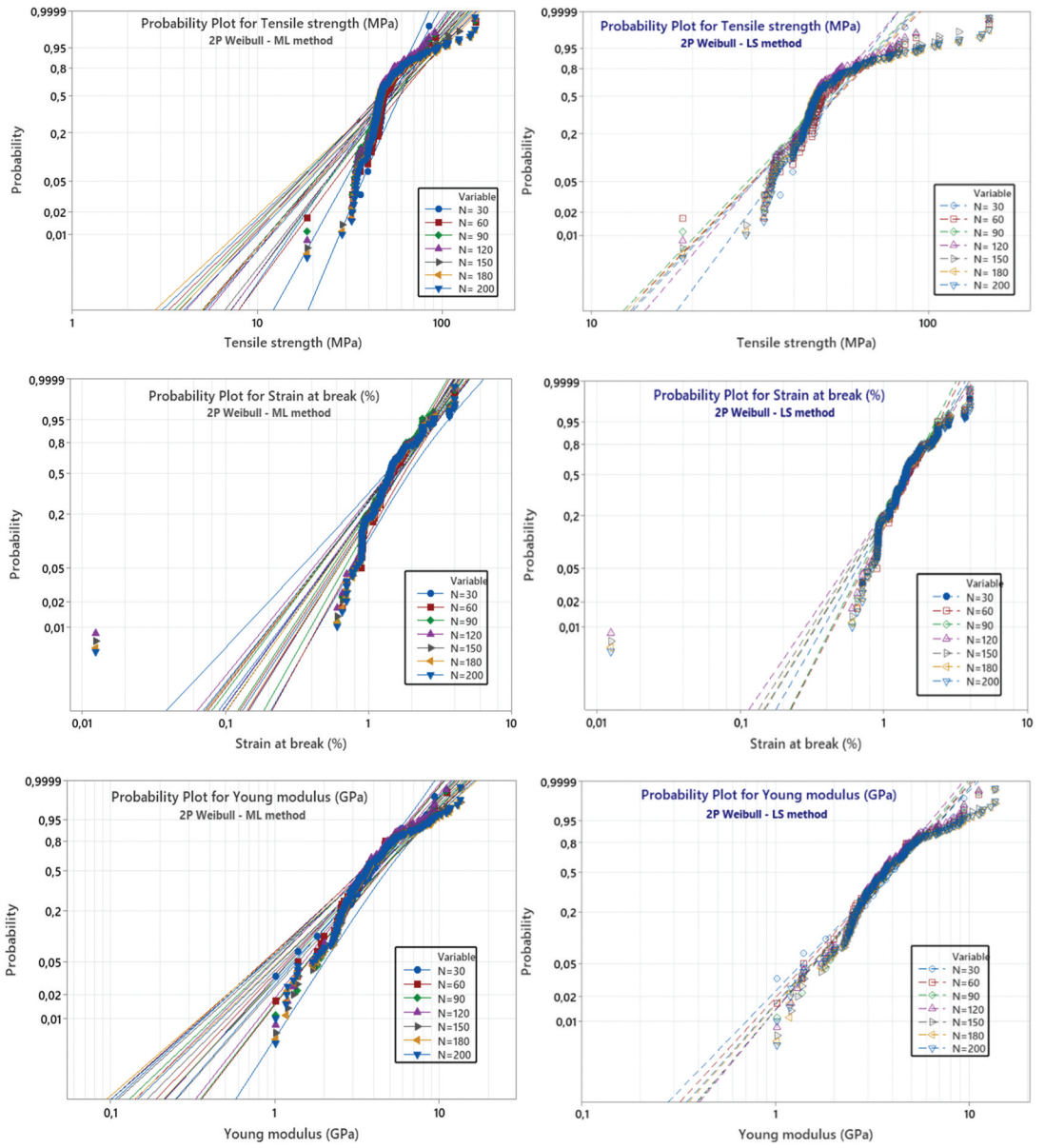

Figure 4. Mechanical properties of AAFS fibers: 2P-Weibull distribution.

modulus of elasticity (m_E) at varying values of N (30, 60, 90, 120, 150, 180, and 200): m_ε values were 2.274, 2.591, 2.612, 2.372, 2.435, 2.412, and 2.352; m_σ values were 4.419, 2.801, 2.846, 2.977, 2.808, 2.483, and 2.547; and m_E values were 2.348, 2.162, 2.243, 2.279, 2.061, 1.951, and 1.976, respectively.

7The probability of survival of mechanical characteristics, specifically tensile resistance, fracture strain, and modulus of elasticity, based on different LS and ML estimation methods, is shown in Figure 5. From this figure, we observe a good alignment with the experimental results. The survival probability was plotted using parameters derived from the Weibull global distribution. The estimating error is nearly negligible, thanks to the availability of a large dataset (200 tests). In Figure 5, the

Table 4. Weibull two-parameter distribution estimates of AAFS fibers with various LS estimators.

	Tensile Strength (MPa)			Strain at break (%)			Modulus of elasticity (GPa)		
N	m_σ	σ_0	R^2	m_ε	ε_0	R^2	m_E	E_0	R^2
Median Rank (Bernard)									
30	6.234	57.21	0.919	3.097	1.81	0.936	2.507	4.67	0.985
60	4.657	58.65	0.908	3.448	1.77	0.959	2.670	4.52	0.975
90	4.735	55.70	0.918	3.498	1.68	0.96	2.884	4.53	0.967
120	5.382	53.78	0.902	2.540	1.76	0.851	2.950	4.35	0.969
150	4.811	56.69	0.896	2.699	1.74	0.859	2.846	4.60	0.958
180	4.659	57.60	0.856	2.776	1.77	0.869	2.722	4.66	0.952
200	4.814	57.39	0.86	2.789	1.78	0.876	2.697	4.65	0.958
Mean Rank (Herd–Johnson)									
30	5.865	57.36	0.923	2.914	1.82	0.941	2.374	4.70	0.983
60	4.507	58.74	0.904	3.315	1.77	0.962	2.572	4.53	0.976
90	4.607	55.78	0.918	3.391	1.68	0.963	2.801	4.54	0.968
120	5.264	53.83	0.901	2.510	1.76	0.841	2.879	4.36	0.971
150	4.715	56.75	0.897	2.671	1.74	0.851	2.787	4.61	0.959
180	4.575	57.67	0.857	2.750	1.77	0.862	2.670	4.67	0.954
200	4.733	57.45	0.861	2.764	1.78	0.87	2.650	4.66	0.96
Modified Kaplan–Meier (Hazen)									
30	6.565	57.08	0.914	3.261	1.80	0.931	2.623	4.65	0.986
60	4.783	58.57	0.91	3.565	1.76	0.956	2.754	4.50	0.973
90	4.843	55.63	0.918	3.589	1.67	0.957	2.954	4.52	0.966
120	5.481	53.73	0.902	2.562	1.76	0.859	3.010	4.34	0.968
150	4.891	56.63	0.896	2.719	1.74	0.867	2.897	4.60	0.956
180	4.730	57.55	0.855	2.794	1.77	0.876	2.765	4.65	0.95
200	4.881	57.34	0.859	2.807	1.78	0.882	2.737	4.65	0.957
Kaplan–Meier									
30	6.033	56.49	0.939	3.002	1.76	0.955	2.476	4.51	0.987
60	4.547	58.16	0.918	3.369	1.75	0.97	2.620	4.45	0.981
90	4.633	55.41	0.928	3.428	1.67	0.969	2.835	4.49	0.973
120	5.277	53.60	0.911	2.540	1.74	0.842	2.905	4.32	0.975
150	4.726	56.53	0.904	2.696	1.73	0.852	2.804	4.58	0.963
180	4.580	57.48	0.863	2.771	1.76	0.864	2.685	4.64	0.957
200	4.737	57.29	0.867	2.782	1.77	0.871	2.663	4.64	0.963

Table 5. Two-parameter Weibull statistics values for AAFS fibers using maximum likelihood method at N200.

	Tensile stress (MPa)			Break strain (%)			Modulus of elasticity (GPa)		
				2P – Weibull – ML method					
N	m_σ	σ_0	σ_u	m_ε	ε_0	ε_u	m_E	E_0	E_u
30	4.419	58.39		2.274	1.87		2.348	4.70	
60	2.801	60.46		2.591	1.81		2.162	4.62	
90	2.846	57.40		2.612	1.72		2.243	4.65	
120	2.977	57.40		2.372	1.76		2.279	4.46	
150	2.808	58.87		2.435	1.75		2.061	4.76	
180	2.483	60.67		2.412	1.78		1.951	4.84	
200	2.547	60.32		2.357	1.80		1.976	4.82	

probability of survival of the traction resistance is depicted and traced using the estimation method of least squares, coupled with Pi = i/n +1. With two sets of parameters from Weibull at *N*= 60, 120 and 180, the values are detailed as: m_σ = 4.547 with σ_0 = 58.16, m_σ = 5.277 with σ_0 = 53.60.19, m_σ = 4.580 with σ_0 = 57.48. Similarly, the results for break strain and modulus of elasticity also display consistency. The Weibull parameter values correspond closely to those cited in the literature for cellulosic fibers (Ahmed Belaadi, Bezazi, Maache, et al. 2014; Bezazi et al. 2014), where the Weibull modulus typically falls between 1.5 and 4.5. Figure 5 further highlights that at a 50% survival probability (P(σ) =

Table 6. ANOVA analysis of the tensile resistance, deformation, and modulus of elasticity of the AAFS fiber at 95% CI.

Source	DF	Seq SS	Contribution	Adj SS	Adj MS	F-Value	P-Value
(A) ANOVA test of tensile strength (N = 30 to 200 tests)							
BG	6	1541	0.51%	1541	256.8	0.71	0.0000645
WG	823	299543	99.49%	299543	364.0		
Total	829	301084	100.00%				
S = 19.0779; R-sq =0.51%; R-sq (adj) = 0.00%; PRESS = 304083; R-sq (pred) = 0.00%.							
(B) ANOVA test of break strain (N = 30 to 200 tests)							
BG	6	0.632	0.17%	0.632	0.1054	0.23	0.000966
WG	823	372.227	99.83%	372.227	0.4523		
Total	829	372.859	100.00%				
S = 0.672518; R-sq =0.17%; R-sq (adj) = 0.00%; PRESS = 378.716; R-sq (pred) = 0.00%.							
(C) ANOVA test of modulus of elasticity (N = 30 to 200 tests)							
BG	6	10.11	0.26%	10.11	1.685	0.36	0.0000904
WG	823	3847.62	99.74%	3847.62	4.675		
Total	829	3857.73	100.00%				
S = 2.16220; R-sq =0.26%; R-sq (adj) = 0.00%; PRESS = 3908.93; R-sq (pred) = 0.00%.							

The terms BG, WG, DF, MS, F, and F-test for ANOVA-one way stand for "between group," "within group," "sum of squares," and "mean square."

0.5) for AAFS fibers, the projected ultimate tensile strength is approximately 39.7 MPa and 36 MPa, respectively, for N=60 and 120. This closely matches the average experimental value calculated at σ = 53.72 MPa. Moreover, the values recorded were 1.59% for strain at failure and 4.25 GPa for modulus of elasticity at P(ε) = P(E) = (0.5).

ANOVA analysis of the AAFS fibers' mechanical characteristics

Statistical methods of data analysis provide a means of improving comprehension and analysis of the experiment's importance. Based on the data's mean and distribution, one-way analysis of variance (ANOVA) was applied in this study to estimate the population samples. According to the first hypothesis, there is no statistical difference between any two-sample means, or they are all the same. Furthermore, the selection of the sample is influenced by the quantity of fibers. P, Fisher's test, MS, SS, and CI were therefore used to perform the ANOVA in order to determine the effect of the test number on these results and to better describe any mechanical property parameters. Table 6 presents the findings from one-way ANOVA for the mechanical properties of AAFS fibers across each of the groups (30, 60, 90, 120, 150, 180, and 200) at a confidence of 95%. Since the p value = 0.000 ($p < .001$) is below the threshold of significance of 0.05, therefore the null hypothesis which assumes that the means would be equal cannot be upheld.

ANN modeling of AAFS fibers

Because of its outstanding performance in feedback networks, the Scaled Conjugate Gradient (SCG) backpropagation algorithm was employed for a system to learn throughout this experiment. Three categories were created from the data utilized in this study's experiments: 20% served for validation, 10% during the test set and data, and 70% were put into the neural network during successive training phases (Figure 6a). For the ANN design that simulated the behavior of AAFS fibers, the SCG was chosen. The ANN model's architecture topology for the behavior of AAFS fibers is shown in Figure 6b. The performance graph illustrates how the errors that are occurring in the network disappear. The progression of each epoch, which can be best understood as the last cycle of the entire neural network information set, was used to determine these mistakes. When the lowest error value is reached, the training immediately ends. Figure 6c demonstrates that, for the tensile behavior of AAFS fibers, the

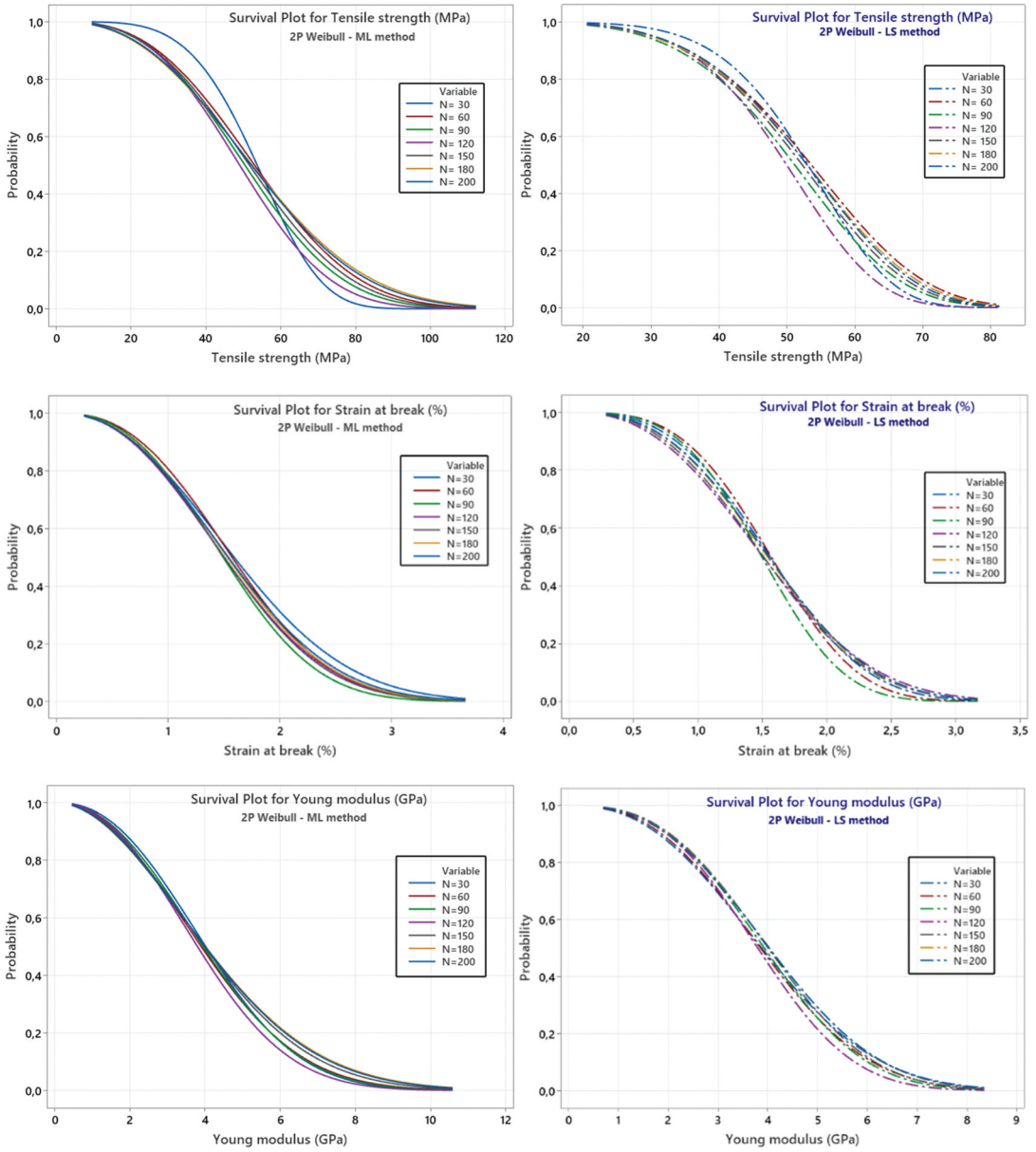

Figure 5. Survival probability plots (using 2P-Weibull) of AAFS fiber mechanical characteristics for ML and LS methods.

average error decreases mostly systematically up to 9 epochs (iterations). In contrast, a supplementary increase in iterations lengthens the training duration while keeping the error quantity constant. This result validates previous research by different investigators on the application of ANN for process modeling and forecasting (Khelifi et al. 2023; Mohit et al. 2023). As seen in Figure 6d, the region of zero error and its vicinity exhibits the fewest mistakes. The minimal error rate of the neural network training stage serves as a sign that the procedure was completed effectively. Based on the determination coefficient (R^2) obtained for training, testing, validation, and all datasets (0.9971, 0.9993, 0.9881, and 0.9939), respectively, as shown in Figure 7a, the network is chosen for model prediction as depicted in Equation (9) with $\varepsilon\text{Tran} = \log((\varepsilon - 0.11)/(1.57 - \varepsilon))$. The best predicting ability of the created model

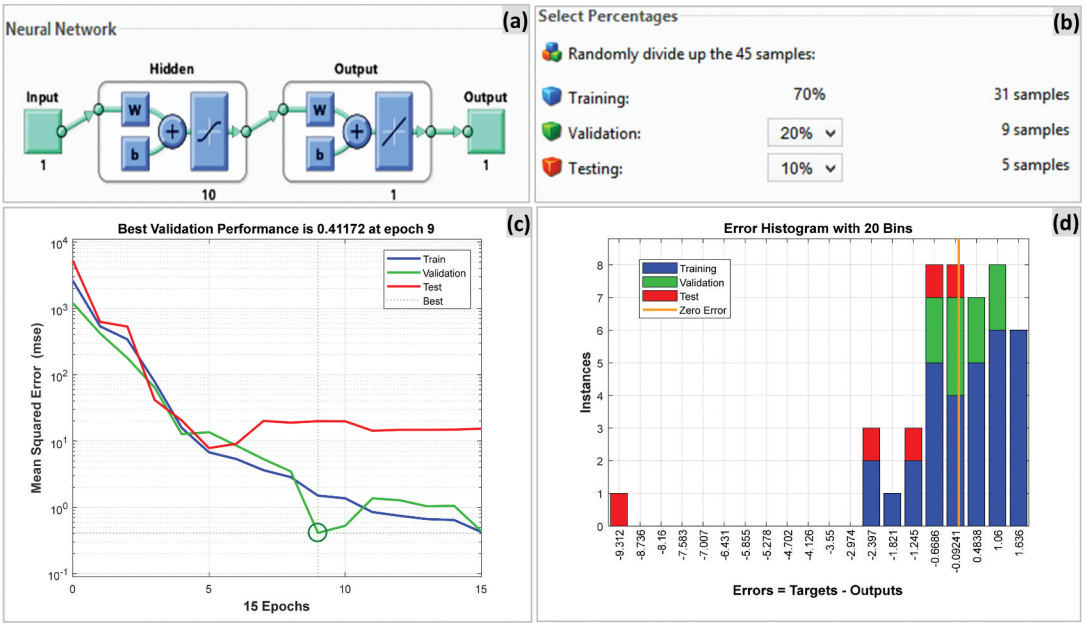

Figure 6. ANN results for the tensile behavior of AAFS fiber (a) data utilized to validate, train, and test samples (b) ANN structure, (c) ANN performance graphs to forecast ideal circumstances and (d) error histogram.

is therefore indicated by the neural network model's more important features in the validation. The testing phase was used to measure the neural network models' accuracy in predicting unknown data.

$$\begin{aligned}\text{ANNresp} = &-1.93 \times H_1 + 4.25 \times H_2 - 3.29 \times H_3 + 3.05 \times H_4 + 2.94 \times H_5 + 5.33 \times H_6 + 2.58 \\ &\times H_7 - 0.05 \times H_8 + 0.07 \times H_9 - 1.58 \times H_{10} + 28.28\end{aligned} \tag{9}$$

$$\begin{cases} H_1 = \tanh(0.5 \times (-0.1608 \times \varepsilon\text{Tran} + 0.3973)) \\ H_2 = \tanh(0.5 \times (1.5327 \times \varepsilon\text{Tran} - 0.8192)) \\ H_3 = \tanh(0.5 \times (-1.3069 \times \varepsilon\text{Tran} + 0.3668)) \\ H_4 = \tanh(0.5 \times (1.3776 \times \varepsilon\text{Tran} - 1.3440)) \\ H_5 = \tanh(0.5 \times (1.2284 \times \varepsilon\text{Tran} - 0.8717)) \\ H_6 = \tanh(0.5 \times (1.7353 \times \varepsilon\text{Tran} - 0.5552)) \\ H_7 = \tanh(0.5 \times (1.0952 \times \varepsilon\text{Tran} - 0.4568)) \\ H_8 = \tanh(0.5 \times (-0.0176 \times \varepsilon\text{Tran} - 0.7487)) \\ H_9 = \tanh(0.5 \times (-0.0937 \times \varepsilon\text{Tran} + 1.7363)) \\ H_{10} = \tanh(0.5 \times (-0.8104 \times \varepsilon\text{Tran} - 0.5327)) \end{cases}$$

To ascertain if the ANN models correctly reflected the non-linear nature of the AAFS fiber behavior, graphic and statistical investigations were conducted. Figure 7b shows a comparison of the ANN models' results with the experimental values. The figures demonstrate a very good fit between the experimental data and all of the proposed response models. Although the ANN was able to evaluate the processes' predictability, the ANN model with 10 hidden neurons proved to be the most effective. The ANN's capacity to handle any kind of non-linearity explains this outcome.

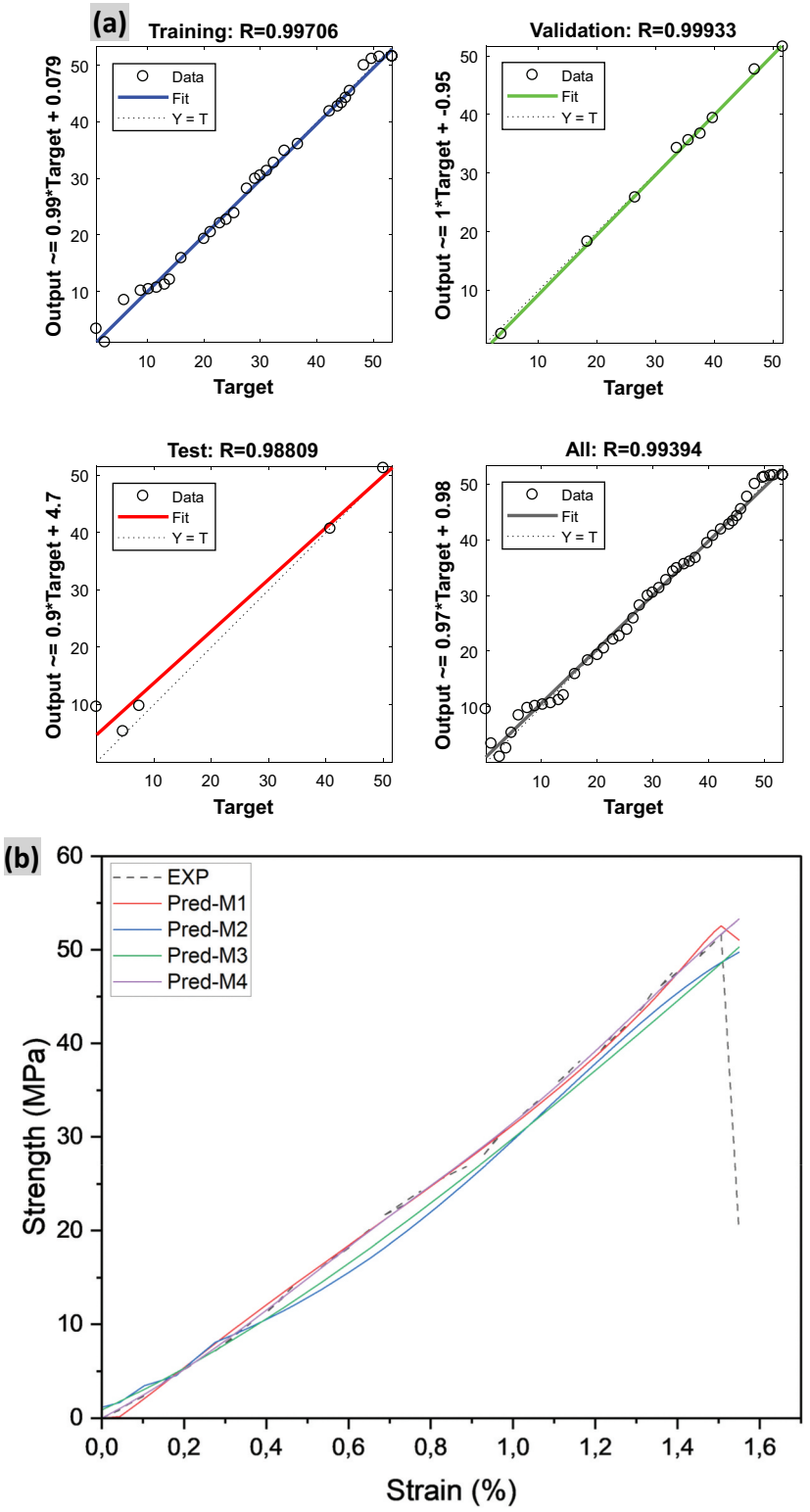

Figure 7. (a) Regression analysis to forecast ideal circumstances and (B) tensile strength curves of AAFS fibers trained using ANN approach.

Conclusions

In order to identify which of the seven tested batches provides the greatest performance, the current work evaluated mechanical parameters such as E, ε, and σ by examining the AAFS fiber condition. The study's primary findings include an increase in the average values of σ and E as well as a rise in batch count from 30 to 200. According to the estimation techniques obtained by LS and ML approaches in the statistical study, it appears that the AAFS fiber is better fitted by Kaplan–Meier estimator. Based on the experimental results, it seems that the fiber AAFS's highest mechanical properties were attained for $N = 180$ trials. In addition, the ANN technique was also used to predict the tensile strength. One-way ANOVA results showed that N exhibited a significant effect on the mechanical characteristics of the AAFS fiber. Regression analysis using artificial neural network demonstrated higher accuracy with a precision of more than 95%. The average experimental tensile behavior data for $N = 180$, which provided the ideal conditions, showed extremely good agreement with the anticipated response patterns. Researchers and designers would find the suggested model to be very useful in obtaining natural fiber-based green composite products.

Highlights

- Agave Americana flower stem fibers (FSAA) are being studied for their potential use in polymer composites.
- Tensile tests were conducted on 200 FSAA fibers.
- The variability of the results was analyzed and quantified using statistical methods and an artificial neural network (ANN).
- The ANN was able to accurately predict the experimental data.
- For each tensile property, the ANOVA test was performed to assess the seven groups.

Acknowledgments

The authors are thankful to the Deanship of Scientific Research at Najran University for funding this work under the Research Groups Funding Program (grant code: NU/RG/SERC/12/24).

Disclosure statement

No potential conflict of interest was reported by the author(s).

Funding

The work was supported by the Deanship of Scientific Research at Najran University [NU/RG/SERC/12/24].

ORCID

Ahmed Belaadi http://orcid.org/0000-0002-6059-3974
Messaouda Boumaaza http://orcid.org/0000-0003-3349-2307

References

Abbasi, B., S. T. A. Niaki, M. A. Khalife, and Y. Faize. 2011. "A Hybrid Variable Neighborhood Search and Simulated Annealing Algorithm to Estimate the Three Parameters of the Weibull Distribution." *Expert Systems with Applications* 38 (1): 700–708. https://doi.org/10.1016/j.eswa.2010.07.022.

Amroune, S., A. Belaadi, M. Bourchak, A. Makhlouf, and H. Satha. 2020. "Statistical and Experimental Analysis of the Mechanical Properties of Flax Fibers." *Journal of Natural Fibers* 19 (4): 1387–1401. https://doi.org/10.1080/15440478.2020.1775751.

Andersons, J., E. Sparniņš, R. Joffe, and L. Wallström. 2005. "Strength Distribution of Elementary Flax Fibres." *Composites Science and Technology* 65 (3–4): 693–702. https://doi.org/10.1016/j.compscitech.2004.10.001.

Andersons, J., E. SparniņŠ, and E. Poriķe. 2009. "Strength and Damage of Elementary Flax Fibers Extracted from Tow and Long Line Flax." *Journal of Composite Materials* 43 (22): 2653–2664. https://doi.org/10.1177/0021998309345035.

Belaadi, A., S. Amroune, and M. Bourchak. 2019. "Effect of Eco-Friendly Chemical Sodium Bicarbonate Treatment on the Mechanical Properties of Flax Fibres: Weibull Statistics." *The International Journal of Advanced Manufacturing Technology* 106 (5–6): 1753–1774. https://doi.org/10.1007/s00170-019-04628-8.

Belaadi, A., S. Amroune, Y. Seki, O. Yasin Keskin, S. Köktaş, M. Bourchak, A. Dufresne, H. Fouad, and M. Jawaid. 2022. "Extraction and Characterization of a New Lignocellulosic Fiber from Yucca Treculeana L. Leaf as Potential Reinforcement for Industrial Biocomposites." *Journal of Natural Fibers* 19 (15): 12235–12250. https://doi.org/10.1080/15440478.2022.2054895.

Belaadi, A., A. Bezazi, M. Maache, and F. Scarpa. 2014. "Fatigue in Sisal Fiber Reinforced Polyester Composites: Hysteresis and Energy Dissipation." *Procedia Engineering* 74:325–328. https://doi.org/10.1016/j.proeng.2014.06.272.

Belaadi, A., M. Bourchak, and H. Aouici. 2016. "Mechanical Properties of Vegetal Yarn: Statistical Approach." *Composites Part B Engineering* 106:139–153. https://doi.org/10.1016/j.compositesb.2016.09.033.

Benzannache, N., A. Belaadi, M. Boumaaza, and M. Bourchak. 2021. "Improving the Mechanical Performance of Biocomposite Plaster/Washingtonian Filifira Fibres Using the RSM Method." *Journal of Building Engineering* 33:101840. https://doi.org/10.1016/j.jobe.2020.101840.

Bezazi, A., A. Belaadi, M. Bourchak, F. Scarpa, and K. Boba. 2014. "Novel Extraction Techniques, Chemical and Mechanical Characterisation of Agave Americana L. Natural Fibres." *Composites Part B Engineering* 66:194–203. https://doi.org/10.1016/j.compositesb.2014.05.014.

Dembri, I., A. Belaadi, M. Boumaaza, and M. Bourchak. 2022. "Tensile Behavior and Statistical Analysis of Washingtonia Filifera Fibers as Potential Reinforcement for Industrial Polymer Biocomposites." *Journal of Natural Fibers* 19 (16): 14839–14854. https://doi.org/10.1080/15440478.2022.2069189.

De Rosa, I. M., J. M. Kenny, D. Puglia, C. Santulli, and F. Sarasini. 2010. "Morphological, Thermal and Mechanical Characterization of Okra (Abelmoschus Esculentus) Fibres as Potential Reinforcement in Polymer Composites." *Composites Science and Technology* 70 (1): 116–122. https://doi.org/10.1016/j.compscitech.2009.09.013.

Elsayed, E. A. 2008. "Reliability Prediction and Accelerated Testing." *Springer Series in Reliability Engineering*. https://doi.org/10.1007/978-1-84800-011-7_7.

Estrada, M., D. L. Linero, and F. Ramírez. 2013. "Constitutive Relationship of the Fiber Cluster of Bamboo Guadua Angustifolia, Determined by Means of a Weibull Probability Function and a Model of Progressive Failure." *Mechanics of Materials* 63 (1): 12–20. https://doi.org/10.1016/j.mechmat.2013.04.007.

Ferfari, O., A. Belaadi, A. Bedjaoui, H. Alshahrani, and M. K. A. Khan. 2023. "Characterization of a New Cellulose Fiber Extracted from Syagrus Romanzoffiana Rachis as a Potential Reinforcement in Biocomposites Materials." *Materials Today Communications* 36 (May): 106576. https://doi.org/10.1016/j.mtcomm.2023.106576.

Fiore, V., T. Scalici, and A. Valenza. 2018. "Effect of Sodium Bicarbonate Treatment on Mechanical Properties of Flax-Reinforced Epoxy Composite Materials." *Journal of Composite Materials* 52 (8): 1061–1072. https://doi.org/10.1177/0021998317720009.

Gahgah, M., A. Belaadi, M. Boumaaza, H. Alshahrani, and M. K. A. Khan. 2023. "Effect of Number of Tests on the Mechanical Characteristics of Agave Sisalana Yarns for Composites Structures: Statistical Approach." *Polymers* 15 (13): 2885. https://doi.org/10.3390/polym15132885.

Indran, S., and R. Edwin Raj. 2015. "Characterization of New Natural Cellulosic Fiber from Cissus Quadrangularis Stem." *Carbohydrate Polymers* 117:392–399. https://doi.org/10.1016/j.carbpol.2014.09.072.

Khelifi, A., M. Boumaaza, A. Belaadi, T. Djedid, A. Azevedo, R. Garcez de, M. Bourchak, and M. Jawaid. 2023. "Effects of Alkaline Treatment of Washingtonia Mesh Waste on the Mechanical and Physical Properties of Bio - Mortar: Experimental and Prediction Models." *Biomass Conversion and Biorefinery*. no. 0123456789. https://doi.org/10.1007/s13399-023-04221-w.

Lalaymia, I., A. Belaadi, A. Bedjaoui, H. Alshahrani, and M. K. A. Khan. 2023. "Extraction and Characterization of Fiber from the Flower Stalk of the Agave Plant for Alternative Reinforcing Biocomposite Materials." *Biomass Conversion and Biorefinery*. https://doi.org/10.1007/s13399-023-04782-w.

Lapidot, I. 2020. "Tech. Report: Modified Kolmogorov – Smirnov Test." *Journal of Biomedical Optics* 25 (4, December): 1–15. https://doi.org/10.13140/RG.2.2.34109.69608.

Lekrine, A., A. Belaadi, A. Makhlouf, S. Amroune, M. Bourchak, H. Satha, and M. Jawaid. 2022. "Structural, Thermal, Mechanical and Physical Properties of Washingtonia Filifera Fibres Reinforced Thermoplastic Biocomposites." *Materials Today Communications* 31:103574. https://doi.org/10.1016/j.mtcomm.2022.103574.

Maache, M., A. Bezazi, S. Amroune, F. Scarpa, and A. Dufresne. 2017. "Characterization of a Novel Natural Cellulosic Fiber from Juncus Effusus L." *Carbohydrate Polymers* 171:163–172. https://doi.org/10.1016/j.carbpol.2017.04.096.

Mohit, H., M. R. Sanjay, S. Siengchin, B. Kanaan, V. Ali, I. M. Alarifi, and M. A. A. E.-B. Tarek. 2023. "Predicting Physico-Mechanical and Thermal Properties of Loofa Cylindrica Fibers and Al2O3/Al-SiC Reinforced Polymer Hybrid Composites Using Artificial Neural Network Techniques." *Construction and Building Materials* 409:133901. https://doi.org/10.1016/j.conbuildmat.2023.133901.

Morris, B. 2003. "The Components of the Wired Spanning Forest are Recurrent." *Probability Theory and Related Fields* 125 (2): 259–265. https://doi.org/10.1007/s00440-002-0236-0.

Mulenga, T. K., A. U. Ude, and C. Vivekanandhan. 2021. "Techniques for Modelling and Optimizing the Mechanical Properties of Natural Fiber Composites: A Review." *Fibers* 9 (1): 6. https://doi.org/10.3390/fib9010006.

Ornaghi, H. L., R. Motta Neves, and F. M. Monticeli. 2021. "Application of the Artificial Neural Network (ANN) Approach for Prediction of the Kinetic Parameters of Lignocellulosic Fibers." *Textiles* 1 (2): 258–267. https://doi.org/10.3390/textiles1020013.

Parida, P. K., A. Kumar Pradhan, and M. Kumar Pandit. 2023a. "Characterization of Cellulose Fiber Extracted from Stems of Myriostachya Wightiana (MW) Plants: A Viable Reinforcement for Polymer Composite." *Fibers and Polymers* 24 (2): 489–503. https://doi.org/10.1007/s12221-023-00020-2.

Parida, P. K., A. Kumar Pradhan, and M. Kumar Pandit. 2023b. "Characterization of Cellulose Fiber Extracted from Stems of Myriostachya Wightiana (MW) Plants: A Viable Reinforcement for Polymer Composite." *Fibers and Polymers* 24 (February): 489–503. https://doi.org/10.1007/s12221-023-00020-2.

Rice, M.-R.-P., T. Meurah, I. Mahlia, N. Saba, A. Hassan, and M. Jawaid. 2019. "Mechanical and Thermal Properties of Montmorillonite-Reinforced Polypropylene/Rice Husk Hybrid Nanocomposites." *Polymers* 11 (10): 11. https://doi.org/10.3390/polym11101557.

Saaidia, A., A. Bezazi, A. Belbah, H. Bouchelaghem, F. Scarpa, and S. Amirouche. 2017. "Mechano-Physical Properties and Statistical Design of Jute Yarns." *Measurement: Journal of the International Measurement Confederation* 111:284–294. https://doi.org/10.1016/j.measurement.2017.07.054.

Sanjay, M. R., P. Madhu, M. Jawaid, P. Senthamaraikannan, S. Senthil, and S. Pradeep. 2018. "Characterization and Properties of Natural Fiber Polymer Composites: A Comprehensive Review." *Journal of Cleaner Production* 172:566–581. Elsevier B.V. https://doi.org/10.1016/j.jclepro.2017.10.101.

Selvaraj, M., P. Chapagain, and B. Mylsamy. 2022. "Characterization Studies on New Natural Cellulosic Fiber Extracted from the Stem of Ageratina Adenophora Plant." *Journal of Natural Fibers* 20 (1). https://doi.org/10.1080/15440478.2022.2156019.

Senthamaraikannan, P., M. R. Sanjay, K. Subrahmanya Bhat, N. H. Padmaraj, and M. Jawaid. 2019. "Characterization of Natural Cellulosic Fiber from Bark of Albizia Amara." *Journal of Natural Fibers* 16 (8): 1124–1131. https://doi.org/10.1080/15440478.2018.1453432.

Van de Velde, K., and P. Kiekens. 1999. "Wettability of Natural Fibres Used as Reinforcement for Composites." *Angewandte Makromolekulare Chemie* 272 (4761): 87–93. https://doi.org/10.1002/(SICI)1522-9505(19991201)272:1<87:AID-APMC87>3.0.CO;2-Q.

Virk, A. S., W. Hall, and J. Summerscales. 2009. "Multiple Data Set (MDS) Weak-Link Scaling Analysis of Jute Fibres." *Composites Part A: Applied Science and Manufacturing* 40 (11): 1764–1771. https://doi.org/10.1016/j.compositesa.2009.08.022.

Virk, A. S., W. Hall, and J. Summerscales. 2010. "Physical Characterization of Jute Technical Fibers: Fiber Dimensions." *Journal of Natural Fibers* 7 (3): 216–228. https://doi.org/10.1080/15440478.2010.504389.

Wang, J., H. Zhou, Z. Liu, X. Peng, and H. Zhou. 2022. "Statistical Modelling of Tensile Properties of Natural Fiber Yarns Considering Probability Distributions of Fiber Crimping and Effective Yarn Elastic Modulus." *Composites Science and Technology* 218:109142. https://doi.org/10.1016/j.compscitech.2021.109142.